

## Preparation and magnetic properties of La<sub>0.9</sub>Ca<sub>0.1</sub>MnO<sub>3</sub> nanoparticles at 300°C

Tianhao Ji, Jiye Fang, Volodymyr Golob, Jinke Tang, and Charles J. O'Connor

Citation: *Journal of Applied Physics* **92**, 6833 (2002); doi: 10.1063/1.1513880

View online: <http://dx.doi.org/10.1063/1.1513880>

View Table of Contents: <http://scitation.aip.org/content/aip/journal/jap/92/11?ver=pdfcov>

Published by the [AIP Publishing](#)

---

### Articles you may be interested in

[Coexistence of considerable inter-particle interactions and spin-glass behavior in La<sub>0.7</sub>Ca<sub>0.3</sub>MnO<sub>3</sub> nanoparticles](#)

*J. Appl. Phys.* **115**, 17B504 (2014); 10.1063/1.4862522

[Magnetic properties and magnetocaloric effect of La<sub>0.8</sub>Ca<sub>0.2</sub>MnO<sub>3</sub> nanoparticles tuned by particle size](#)

*J. Appl. Phys.* **111**, 063922 (2012); 10.1063/1.3699037

[Dynamic properties of cluster glass in La<sub>0.25</sub>Ca<sub>0.75</sub>MnO<sub>3</sub> nanoparticles](#)

*J. Appl. Phys.* **106**, 083904 (2009); 10.1063/1.3246869

[Nanoparticle size effect on the magnetic and transport properties of \(La<sub>0.7</sub>Sr<sub>0.3</sub>\)<sub>0.9</sub>Mn<sub>1.1</sub>O<sub>3</sub> manganites](#)

*Low Temp. Phys.* **35**, 568 (2009); 10.1063/1.3170933

[Comparison of magnetotransport properties of nano- and microcrystalline La<sub>0.7</sub>Ca<sub>0.3</sub>MnO<sub>3</sub> manganites in high magnetic field](#)

*J. Appl. Phys.* **104**, 123902 (2008); 10.1063/1.3040013

---



**Not all AFMs are created equal**  
**Asylum Research Cypher™ AFMs**  
**There's no other AFM like Cypher**

[www.AsylumResearch.com/NoOtherAFMLikeIt](http://www.AsylumResearch.com/NoOtherAFMLikeIt)

**OXFORD**  
INSTRUMENTS  
*The Business of Science®*

# Preparation and magnetic properties of $\text{La}_{0.9}\text{Ca}_{0.1}\text{MnO}_3$ nanoparticles at 300 °C

Tianhao Ji, <sup>a)</sup> Jiye Fang, Volodymyr Golob, Jinke Tang, and Charles J. O'Connor  
*Advanced Material Research Institute, University of New Orleans, New Orleans, Louisiana 70148*

(Received 27 June 2002; accepted 21 August 2002)

Nanosized  $\text{La}_{0.9}\text{Ca}_{0.1}\text{MnO}_3$  perovskite-type crystalline complex oxides have been prepared at the low calcination temperature of 300 °C. The preparation procedure was carried out by the two-step process of amorphous formation and calcination. The amorphous phase was obtained by the reaction of metal ions with tetrabutylammonium hydroxide at 245 °C, and then calcined at 300 °C (sample A) or 400 °C (sample B) to prepare the nanocrystalline materials. The magnetic measurement shows that spin-glass behavior exists at 45 K and the blocking temperature increases with an increase of calcination temperature. The result of the spin-glass temperature of 45 K demonstrates that the particle size of the two samples A and B is below 50 nm. The increase of blocking temperature from A to B indicates that the particle size of A is less than that of B. The measurement of the normalized resistivity versus temperature for samples A and B shows that they have the change of the normalized resistive value at 230 K. © 2002 American Institute of Physics.  
[DOI: 10.1063/1.1513880]

## I. INTRODUCTION

Perovskite-type  $\text{Ln}_{1-x}\text{A}_x\text{MnO}_3$  (A representing divalent cations such as Ca, Sr, or Ba) compounds have been of interest for many years due to their special magnetotransport properties.<sup>1-4</sup> As  $\text{Ln}^{3+}$  metal ions were partially replaced by divalent ions  $\text{A}^{2+}$ , a mixed  $\text{Mn}^{3+}/\text{Mn}^{4+}$  valence was observed. The magnetic coupling between neighboring  $\text{Mn}^{3+}$  and  $\text{Mn}^{4+}$  ions (double exchange) results in metallic conductivity and ferromagnetic characteristics.<sup>5-7</sup> When the size of this kind of material becomes nanometer scale, their properties obviously change. For example, the temperature dependence of magnetoresistance is improved and the onset of the freezing behavior of surface spin-glass takes place at 45 K when the nanoparticle size is below 50 nm.<sup>8</sup> As these nanoparticles are prepared above 500 °C,<sup>9</sup> they connect strongly with each other and the capping ligand on the surface of nanoparticles. In order to study the effect of the capping ligand on the resistivity of  $\text{La}_{0.9}\text{Ca}_{0.1}\text{MnO}_3$  (LCMO) nanoparticles and further demonstrate the feature of surface spin-glass, we used another preparation method at 300 °C to obtain LCMO nanoparticles. In general, chemical methods such as sol-gel<sup>9</sup> and metal complex decomposition<sup>10</sup> have been used to prepare this kind of nanoparticle. Herein we report the preparation of LCMO nanoparticles at lower temperature and the freezing temperature of spin-glass behavior at 45 K.

The preparation procedure was performed by the two-step process of amorphous formation and calcination. The first step is the formation of the LCMO amorphous phase, and further, the LCMO nanocrystal is obtained by low-temperature calcinations in the air. Magnetization measurement demonstrated that the onset of freezing temperature of spin-glass behavior is at 45 K.

## II. EXPERIMENTAL DETAILS

### A. Starting materials

The chemicals used in this work include: lanthanum nitrate hexahydrate [ $\text{La}(\text{NO}_3)_3 \cdot 6\text{H}_2\text{O}$ , >99%, Aldrich], calcium chloride ( $\text{CaCl}_2$ , Aldrich), manganese chloride ( $\text{MnCl}_2 \cdot 4\text{H}_2\text{O}$ , reagent grade, Matheson Coleman & Bell), diethylene glycol (99%, Alfa Aesar), and tetrabutylammonium hydroxide (1.0 M solution in methanol, Aldrich).

### B. Experimental procedure

The LCMO nanocrystals were prepared by an amorphous-calcination two-step synthesis route. First, the lanthanum nitrate hexahydrate, calcium chloride, and manganese chloride were added into 150 mL of diethylene glycol, respectively. The temperature was raised to about 120 °C and the solution was stirred for 1 h. After the metal salts were dissolved, tetrabutylammonium hydroxide (TBAH) was rapidly added and stirring of the solution was continued for one additional hour. The solution was heated to 245 °C and refluxed for 12 h. After cooling to room temperature, the brown colloidal particles were separated by centrifugation. The particles were then redispersed into ethanol, sonicated for 5 min, and separated again from the liquid. By repeating this procedure four times, the amorphous LCMO phase was obtained. After the amorphous material was calcinated at 300 °C in the air for 10 h, the LCMO nanocrystal was obtained.

X-ray powder diffraction (XRD) data were obtained at room temperature using a Philips X'Pert-MPD. The thermogravimetric analysis (TGA) was carried out on a TA Instruments Thermal Analyst 2000 System. The magnetic measurements were performed by using a Quantum Design MPMS-5S superconducting quantum interference device magnetometer. The resistivity of two pellet samples was

<sup>a)</sup>Electronic mail: tji@uno.edu

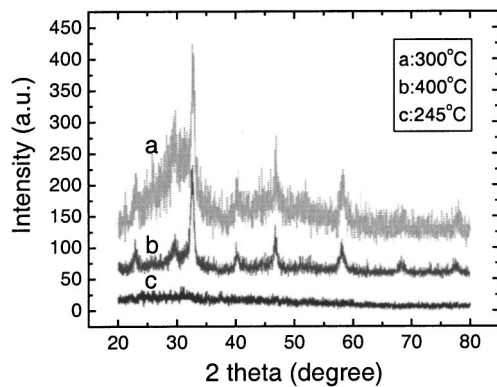


FIG. 1. XRD pattern of the  $\text{La}_{0.9}\text{Ca}_{0.1}\text{MnO}_3$  nanoparticles prepared at calcinations temperature 300 °C (a), 400 °C (b), and the amorphous phase (c).

measured using a Quantum Design Physical Properties Measurement System (PPMS).

### III. RESULTS AND DISCUSSION

Metal hydroxide was first formed by using the organic base TBAH at low temperature. Further, at a distillation temperature of 245 °C, an amorphous phase demonstrated by an XRD pattern [Fig. 1(c)] was prepared.  $\text{TBA}^+$  as capping ligand cation bound onto the surface of the amorphous phase, and this amorphous material can be separated easily from the alcohol solvent. Then the amorphous powder was centrifuged and washed four times with anhydrous ethanol. After the dried amorphous material was heated at 300 °C [Fig. 1(a), sample A] and 400 °C [Fig. 1(b), sample B] in the air, respectively, the perovskite-type LCMO was obtained. From this figure, the crystalline size was estimated by applying the Scherrer equation as follows:

$$D = (57.3 k \lambda) / (\beta \cos \theta),$$

where  $k$  is particle shape factor (generally taken as 0.9),  $\lambda$  the wavelength of  $\text{Cu K}\alpha_1$  radiation (1.540 56 Å),  $\beta$  the calibrated half intensity width of the selected diffraction peak (degrees),  $\theta$  the Bragg angle (half of the peak position angle),  $D$  the crystallite size, and the factor 57.3 is used to convert  $\beta$  in degree to radian measurement. From the equation the average size of the samples A and B was about 11 and 15 nm, respectively.

The TGA measurements were performed in a flow of air. The TGA results for the amorphous powder (Fig. 2) show different regions of weight loss as observed in the TGA curve with the increase of temperature from room temperature to 700 °C at the rate of 10 °C per min. The first region from room temperature to 230 °C corresponds to the loss of absorbed organic molecular ethyl alcohol and the dehydration reaction of hydroxide. The second region of weight loss from 230 to 250 °C is due to the desorption of diethylene glycol (boiling point 245 °C). Although the hydroxide dehydration reaction of metal ions took place at 245 °C to form the amorphous phase, a crystalline structure was not formed yet.

Figure 3 shows the temperature dependence of the magnetization via zero-field-cooled (ZFC) and field-cooled (FC)

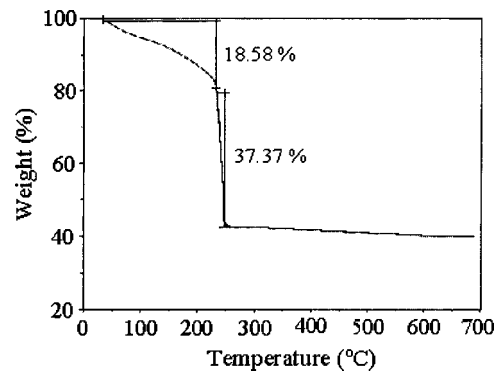


FIG. 2. TGA of the amorphous phase which was heated from room temperature to 700 °C in a flow of air.

processes with an applied field of 50 Oe for the two LCMO samples. The ZFC curves in Figs. 3(a) and 3(b) exhibit a typical blocking process with the blocking temperature at 150 and 160 K, respectively. As the two powders were not pressed under pressure, the interaction energy between particles is assumed not to change.<sup>11</sup> The blocking temperature ( $T_B$ ) is given as follows:

$$T_B = E_a / k_B \ln(tf_0),$$

where  $E_a$  is the anisotropy barrier that can be determined by  $E_a = KV$  in which  $K$  is the anisotropy energy density constant and  $V$  is the volume of particle;  $t$  is the experimental measuring time and  $k_B \ln(tf_0)$  can be treated as a constant.<sup>12–14</sup> Thus generally  $T_B$  increases with an increase

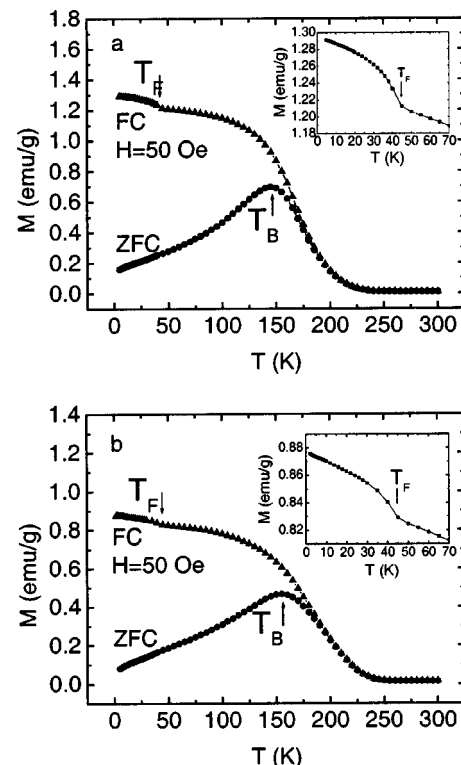


FIG. 3. Temperature dependence of low-field ZFC-FC magnetization of the nanosized  $\text{La}_{0.9}\text{Ca}_{0.1}\text{MnO}_3$  for two samples A and B is shown. Insets are the detail of the FC branch for samples A and B showing the sudden decrease of the magnetization at about 45 K.

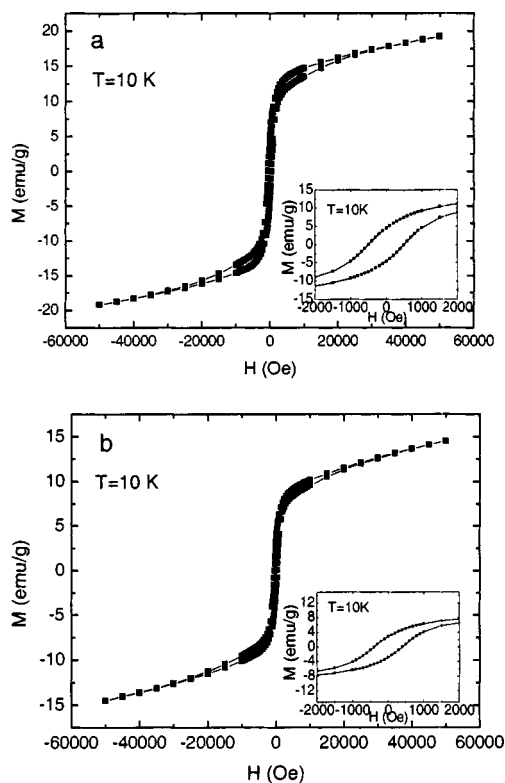


FIG. 4. Hysteresis loops of the two samples A and B. Insets are the enlargement of the hysteresis loops in the applied field range  $\pm 2$  kOe. From the insets we can clearly observe the coercivity and remnant magnetization of samples A and B.

of V. This result indicates that the particle size for the calcined sample at  $400^\circ\text{C}$  (sample B) is bigger than that of the sample calcined at  $300^\circ\text{C}$  (sample A). At the same time, the FC curves reveal the existence of a sudden increase of the magnetization of the two samples at the same temperature  $T_F = 45$  K, in agreement with the literature.<sup>8,15</sup> This is because the surface spin-glass layer of the two nanosized LCMO is suddenly frozen. As the spin-glass-like transition disappears for particle size above 50 nm, this result further demonstrates that the nanoparticle size for the two samples is below 50 nm, in agreement with the calculation of the Scherrer equation from the XRD pattern.<sup>8</sup> Additionally we did not observe monodisperse nanoparticle size due to the connection of particles calcined at high temperature.

Figure 4 shows the hysteresis loop at 10 K for the two samples. From Fig. 4(a), the coercivity and remnant magnetization for sample A are 19 emu/g, 500 Oe and 5 emu/g, but for sample B, 14 emu/g, 400 Oe and 2.5 emu/g, respectively. Generally magnetization and coercivity of LCMO material are dependent on the composition of divalent cation A,<sup>16,17</sup> temperature,<sup>18</sup> lattice effect,<sup>19</sup> and particle size.<sup>8</sup> Because we use the same composite sample to measure the hysteresis loop under the same condition, the magnetization and coercivity only depend on lattice effects and particle size. Although the above results demonstrate that the nanoparticle size of sample A is less than that of sample B, which would lead to larger magnetization and coercivity of sample B,<sup>10</sup> on the contrary, the magnetization and coercivity of sample A are larger. It may be explained from the lattice effect due to

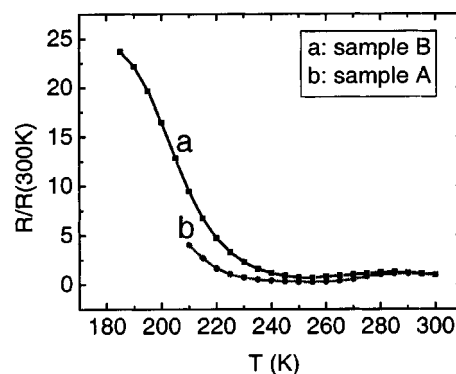


FIG. 5. Temperature dependence of the normalized resistivity  $R(T)/R(300\text{ K})$  for the two samples A and B.

a strong Jahn–Teller electron phonon coupling.<sup>19,20</sup> At low calcination temperature, sample A might have a much more remarkable distortion of the surrounding lattice.

The calcinated powder of the two samples was pressed into pellets under the same high pressure so that they could be measured for the temperature dependence of resistivity. Figure 5 shows the temperature dependence of the normalized resistivity  $[R(T)/R(300\text{ K})]$  for the two pellets. From the curves the normalized resistive value has obvious change at 230 K and below this temperature the sample B has a bigger value than that of the sample A. Lower temperatures could not be measured because the resistivity value of samples A and B extended beyond the measurement range of the instrument.

#### IV. CONCLUSIONS

The  $\text{La}_{0.9}\text{Ca}_{0.1}\text{MnO}_3$  nanoparticles have been prepared at  $300^\circ\text{C}$  by a two-step amorphous-calcination synthesis route. The results of magnetic analysis show that a freezing temperature ( $T_F$ ) due to spin-glass behavior is observed at 45 K, which demonstrates that the particle size of samples A and B is below 50 nm and the blocking temperature ( $T_B$ ) shifts from 150 to 160 K with the increase of calcination temperature from 300 to  $400^\circ\text{C}$ . We propose that the Jahn–Teller effect causes the magnetization and coercivity of sample A to be larger than those of sample B. The measurement of the normalized resistivity versus temperature for samples A and B shows that they have the change of the normalized resistive value at 230 K.

#### ACKNOWLEDGMENTS

The authors are grateful to Dr. A. Vovk and Dr. V. Kolesnichenko for the help with this experiment. The authors also thank Dr. G. Carunto, Dr. J. He, and Dr. W. Zhou for the help with the TGA and TEM measurement. The authors gratefully acknowledge the support of this work by the Advanced Material Research Institute (AMRI) through the Louisiana Board of Regents Contract No. NSF/LEQSF(2001-04)-R11-03.

<sup>1</sup>C. N. R. Rao and A. K. Cheetham, *Science* **272**, 369 (1996).

<sup>2</sup>Z. Wang, T. Ji, Y. Wang, X. Chen, R. Li, J. Cai, J. Sun, and B. Shen, *J. Appl. Phys.* **87**, 5582 (2000).

- <sup>3</sup>A. J. Millis, *Nature (London)* **392**, 147 (1998).
- <sup>4</sup>H. D. Hudspeth, F. Sharifi, I. J. Guilaran, P. Xiong, and S. von Molar, *Phys. Rev. B* **65**, 052405 (2002).
- <sup>5</sup>C. Zener, *Phys. Rev.* **82**, 403 (1951).
- <sup>6</sup>P. W. Anderson and H. Hasegawa, *Phys. Rev.* **100**, 675 (1955).
- <sup>7</sup>H. Kubo and N. Ohata, *J. Phys. Soc. Jpn.* **33**, 21 (1972).
- <sup>8</sup>T. Zhu, B. G. Shen, J. R. Sun, H. W. Zhao, and W. S. Zhan, *Appl. Phys. Lett.* **78**, 3863 (2001).
- <sup>9</sup>R. Mahesh, R. Mahendiran, A. K. Raychaudhuri, and C. N. R. Rao, *Appl. Phys. Lett.* **68**, 2291 (1996).
- <sup>10</sup>T. Yi, S. Gao, X. Qi, Y. Zhu, F. Cheng, B. Ma, Y. Huang, C. Liao, and C. Yan, *J. Phys. Chem. Solids* **61**, 1407 (2000).
- <sup>11</sup>J. Dai, J. Wang, C. Sangregorio, J. Fang, E. Carpenter, and J. Tang, *J. Appl. Phys.* **87**, 7397 (2000).
- <sup>12</sup>M. El-Hilo, K. O'Grady, and R. Chantrell, *J. Magn. Magn. Mater.* **114**, 295 (1992).
- <sup>13</sup>D. A. Dimitrov and G. M. Wysin, *Phys. Rev. B* **54**, 9237 (1996).
- <sup>14</sup>D. L. Leslie-Pelecky and R. D. Chakoumakos, *Chem. Mater.* **8**, 1770 (1996).
- <sup>15</sup>S. Lee, H. Y. Hwang, B. I. Shraiman, W. D. Ratcliff, and S. W. Cheong, *Phys. Rev. Lett.* **82**, 4508 (1999).
- <sup>16</sup>T. I. Arbutova, I. B. Smolyak, S. V. Naumov, A. A. Samokhvalov, and A. V. Korolev, *J. Exp. Theor. Phys.* **92**, 100 (2001).
- <sup>17</sup>R. Laiho, K. G. Lisunov, E. Lahderanta, P. Petrenko, J. Salminen, V. N. Stamov, and V. S. Zakhvalinskii, *J. Phys.: Condens. Matter* **12**, 5751 (2000).
- <sup>18</sup>R. Laiho, K. G. Lisunov, E. Lahderanta, P. Petrenko, V. N. Stamov, and V. S. Zakhvalinskii, *J. Magn. Magn. Mater.* **213**, 271 (2000).
- <sup>19</sup>A. J. Millis, P. R. Littlewood, and B. I. Shraiman, *Phys. Rev. Lett.* **74**, 5144 (1995).
- <sup>20</sup>L. Zheng, K. Li, and Y. Zhang, *Phys. Rev. B* **58**, 8613 (1998).